

Key Features in the Measured Band Structure of $\text{Bi}_2\text{Sr}_2\text{CaCu}_2\text{O}_{8+\delta}$: Flat Bands at E_F and Fermi Surface Nesting

D. S. Dessau,¹ Z.-X. Shen,^{1,2} D. M. King,¹ D. S. Marshall,¹ L. W. Lombardo,² P. H. Dickinson,²
A. G. Loeser,¹ J. DiCarlo,¹ C.-H. Park,¹ A. Kapitulnik,² and W. E. Spicer¹

¹*Solid State Laboratories, Stanford University, and Stanford Synchrotron Radiation Laboratories, Stanford, California 94305*

²*Department of Applied Physics, Stanford University, Stanford, California 94305*

(Received 16 March 1993)

The near- E_F electronic structure and Fermi surface of $\text{Bi}_2\text{Sr}_2\text{CaCu}_2\text{O}_{8+\delta}$ have been mapped out with angle-resolved photoemission. Key features of the measured band structure are (1) an extended region of flat CuO_2 derived bands very near E_F and (2) a strong propensity for Fermi surface nesting. Comparative analysis of these data with those from other cuprate superconductors suggests that these features may be responsible for many of the anomalous physical properties of the p -type cuprates, while the absence of these features may be related to the more "normal" physical properties of the n types.

PACS numbers: 71.20.Cf, 74.72.Hs, 79.60.Bm

A microscopic theory of high-temperature superconductivity requires an understanding of the electronic structure near the Fermi level. Many of the unusual physical properties including the anomalously high T_c have often been attributed to particular characteristics of the low energy excitations determined by the electronic structure. However, despite the large body of existing transport and spectroscopic data, experiment has not yet isolated the key elements of the electronic structure necessary for a global understanding of the physical properties of the cuprates. Through a thorough angle-resolved photoemission study of high quality single crystals of the $\text{Bi}_2\text{Sr}_2\text{CaCu}_2\text{O}_{8+\delta}$ (Bi 2212) compound, the only cuprate superconductor known to have a surface representative of the bulk [1], we have found features in the electronic structure that may prove very important for understanding many of the anomalous physical properties of the cuprate superconductor.

The most striking aspect of the experimental data is a set of very flat bands close to E_F in an extended \mathbf{k} -space region centered around the \bar{M} point. The presence of these flat bands at E_F in the p -type cuprates Bi 2212, $\text{Bi}_2\text{Sr}_2\text{CuO}_6$ (Bi 2201), and $\text{YBa}_2\text{Cu}_3\text{O}_y$ (YBCO) and the absence of these flat bands at E_F in the n -type cuprate $\text{Nd}_{2-x}\text{Ce}_x\text{CuO}_4$ (NCCO) appear to be correlated to the very different physical properties observed in these two classes of materials. This suggests that the flat bands at E_F may be a key to understanding many of the unusual physical properties observed in the p -type cuprates. Some very strong renormalizations or more exotic theories [2] are needed to account for these flat bands, as their presence near E_F in such an extended \mathbf{k} -space region cannot be accounted for by the local-density approximation (LDA) band theory calculations. In addition to the flat bands at E_F , we present the most detailed experimental Fermi surface (FS) information of a high- T_c compound. The most noteworthy aspect of the measured FS is the very strong tendency for nesting, a fact which also may be important for understanding many of the unusual physical properties of Bi 2212 and related com-

pounds. In particular, a nesting vector \mathbf{Q} near (π, π) exists in Bi 2212 but is absent in NCCO; this may be related to the momentum dependence of the dynamical susceptibility and of the order parameter in Bi 2212 [3].

A single crystal [4] of Bi 2212 with a Meissner T_c of 85 K and transition width of 1 K was transferred into our experimental chamber without baking, and cleaved *in situ* in a vacuum of 1×10^{-10} torr. Linearly polarized photons of energy 20.5 eV were provided by the SSRL undulator beam line 5, with the ejected photoelectrons collected and energy analyzed by a Vacuum Science Workshops HA50 system modified for multichannel detection. The combined (electron and photon) energy resolution of the experimental system was approximately 45 meV (higher resolution was available, but was sacrificed in order to obtain counting rates sufficient to take the great number of spectra necessary for the experiment), and the angular resolution of the electron spectrometer was $\pm 1^\circ$. For the measurements reported here, the sample was held at a temperature of 100 K, comfortably above the 85 K T_c . Even though the measurements took an entire week to complete, no damaging aging effects such as the -9 eV "dirt" peak or a loss of Fermi level intensity were ever detected, confirming the excellent stability of the cleaved Bi 2212 surface [5]. The results presented here have been qualitatively reproduced on a large number of similar crystals.

Figure 1(a) shows a set of normalized [6] near- E_F spectra taken along the Γ - X high symmetry direction, with the exact \mathbf{k} -space location of each spectrum within the cut as indicated in Fig. 2(a). For our purposes, we can think of the spectra as being made up of two parts: a dispersive feature (quasiparticle peak) with peak locations marked by the triangles, and a \mathbf{k} -independent "background" extending up to E_F which the quasiparticle peak rides upon [7]. As the lifetime of the state is a function of its energy, the peak narrows and grows in height as it approaches E_F . With continued dispersion, the peak reaches and finally crosses E_F , rapidly decreasing in intensity in the process. At the emission angle of θ/ϕ

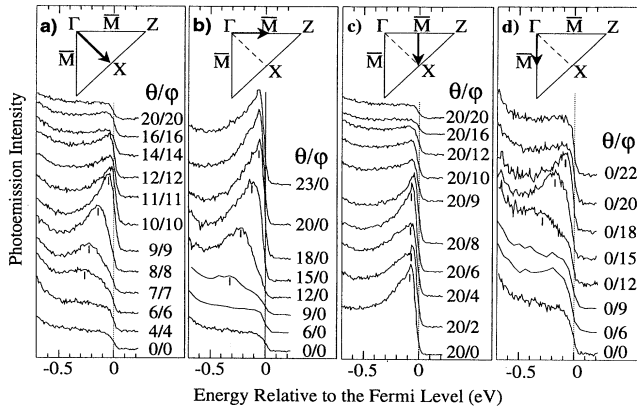


FIG. 1. Near- E_F normal state ($T=100$ K) ARPES data from a $T_c=85$ K Bi 2212 crystal. θ/ϕ is the emission angle in degrees relative to the sample normal. The arrows in the insets show the general direction of each cut within the Brillouin zone.

$=10^\circ/10^\circ$, the peak has approximately half its maximum strength above the background and the Fermi energy lies near the midpoint of the leading edge. This indicates that this is the location of the FS crossing. This crossing is indicated in Fig. 2(a) by the dark shading of the circle at 10/10.

Three other representative cuts through the Brillouin zone are shown in panels (b) through (d) of Fig. 1. The cut of panel (b), taken along the Γ - \bar{M} zone diagonal, shows a peak dispersing towards and then skimming very near E_F for emission angles beyond $\theta/\phi=15/0$. Since the peak does not show a strong intensity modulation as it remains near E_F , we cannot distinguish a FS crossing. All we can infer is that a band is very near E_F (probably within ± 30 – 50 meV) throughout this region. This is indicated in Fig. 2(a) by the diagonally striped circles. The cut of Fig. 1(c) shows the behavior of these states as we move from near \bar{M} towards X . The near- E_F peak at 20/0 remains essentially unchanged until near 20/8, where the intensity begins to dramatically decrease, signaling a FS crossing. As we can see from Fig. 2(a), there is a peak near E_F for a very large portion of the Brillouin zone.

Figure 1(d) shows a cut along Γ - \bar{M} taken by varying the ϕ emission angle. Surprisingly, this cut shows a clear FS crossing, even though panel (b) (taken along a crystallographically equivalent direction) did not show the crossing. To determine the cause of this, we rotated the sample by 90° (leaving the direction of polarization of the incident light fixed) and retook some of the cuts. A comparison with the unrotated spectra indicated that the lack of symmetry is due to matrix element differences associated with the photon polarization direction relative to the electron emission direction, and not a result of any broken symmetry of the crystal itself. These polarization effects proved to be an especially valuable tool in the deconvolution of the band structure [8]. More details of the polarization effects, as well as the complete set of

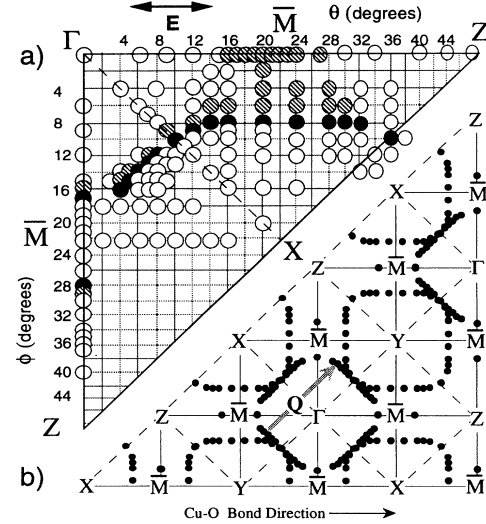


FIG. 2. (a) A summary of all the cuts taken. Each measurement is denoted by a circle, with the size of the circle denoting the \mathbf{k} resolution of the experiment. Filled circles correspond to Fermi-surface crossings and striped circles to locations where the band energy is indistinguishable from E_F . (b) The experimental Fermi surface obtained by reflecting the crossing points (dark circles) of (a) around the high symmetry directions. A nesting vector \mathbf{Q} near (π, π) is shown.

data that went into Fig. 2(a), will be presented in an upcoming publication.

Figure 2(b) shows the experimentally determined FS obtained by reflecting the crossing points of 2(a) around the high symmetry axes. We observed two strongly nested pieces of FS—one centered around the $X(Y)$ point and one centered around the Γ point (and presumably also around the Z point). This very strong nesting may be important for understanding the quasiparticle scattering in these materials [3] as well as the unusual temperature variations of the Hall coefficient and Hall angle in Bi 2212 and YBCO that have been explained in terms of an anisotropic damping that is a function of the curvature of the FS [9]. In addition, the fact that there is a nesting vector \mathbf{Q} near (π, π) may help explain why the measured dynamical susceptibility $\chi(q, \omega)$ is so strongly peaked near the wave vector (π, π) [3]. We also note that a susceptibility with this wave vector dependence favors a $d_{x^2-y^2}$ pairing channel, a result consistent with the gap anisotropy found by us on the same compound [10] and with theories of superconductivity based upon antiferromagnetic spin fluctuations [11].

The experimental E vs \mathbf{k} relationship along the high symmetry directions is shown in Fig. 3. The circles represent the experimental data points, while the lines represent our best interpretation of the dispersion relationships. Because we observe two distinct pieces of FS in Fig. 2, we show two bands, one each from the even and odd combinations of the two CuO_2 planes per unit cell.

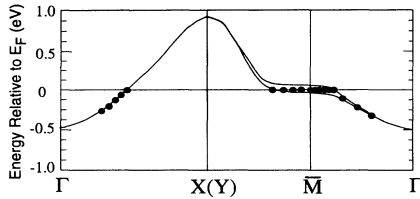


FIG. 3. Experimental E vs \mathbf{k} relationship along various high symmetry directions (points). The lines illustrate a simple scenario compatible with the data.

One of these bands crosses E_F between Γ and \bar{M} and one crosses between \bar{M} and $X(Y)$, as in Fig. 2. The bands are in general nondegenerate, except along Γ - $X(Y)$ where the splitting appears to be small or zero, in agreement with the predictions of LDA calculations [12]. The fact that we have not definitively observed these two separate bands in any one spectrum is, we feel, principally due to the strong selection rules as a function of polarization as well as the rapid broadening and weakening of the quasiparticle peaks as a function of energy. We note that the above interpretation of the data is not unique; Anderson has proposed an explanation of the data that does not require intracellular coupling but instead relies on both real and “ghost” pieces of FS. In this theory, the ghost FS’s exist due to the proposed composite nature of the electronic excitations in two dimensions, and explain the large \mathbf{k} -space region of quasiparticle weight at E_F [2].

The band structure and FS of Bi 2212 have been calculated by a number of groups using the local-density band theory approximation. The calculations in general show two large nearly degenerate pieces of CuO_2 FS centered around the $X(Y)$ points, as well as a small piece of FS with strong BiO character. These calculations do not agree well with the experimental data. Massida *et al.* have done an additional calculation in which the interaction between the BiO states and the CuO_2 states has been artificially ignored, and find two pieces of CuO_2 FS which are very similar to the measured FS of Fig. 2(b) [12]. This implies that the electronic states near E_F are mainly CuO_2 derived, and the BiO bands remain entirely above E_F for all \mathbf{k} . This scenario is consistent with that from tunneling experiments, which have found the Bi-O plane to be nonmetallic [13]. Of course, a slight amount of BiO-CuO hybridization is still expected [14]. Possible explanations as to why the band calculation incorrectly predicted the BiO potential are the nonstoichiometry of the compound and the superstructure in the BiO planes.

The experimental electronic structure near E_F (and thus the low energy quasiparticle excitation spectra) diverges even more from the band theory than does the FS. The most striking aspect of the data of Fig. 3 is the presence of the flat bands in a very significant portion of the Brillouin zone that cannot be explained by either of the band theory scenarios. The experiment reveals two bands within 30–50 meV of E_F around the \bar{M} point. The

calculation which ignores the BiO- CuO_2 interaction shows what appears to be these same two bands, yet they show much greater dispersion near the \bar{M} point and a much greater energy splitting. These differences may imply that the correlation effects which are responsible for the renormalization are much greater near \bar{M} than along Γ - $X(Y)$ where a mass enhancement (relevant to the LDA result) of a factor of 2 is observed [15]. In fact, it has been suggested that the correlations are so strong that the concept of a quasiparticle may no longer be relevant, and the flat bands at E_F in such an extended \mathbf{k} -space region are a signature of non-Fermi-liquid behavior in a confined CuO_2 plane [2].

Regardless of the origin of these flat bands, the key point is that they are found very near E_F for all of the p -type cuprates successfully measured to date (Bi 2212, Bi 2201, Y 123, and Y 124) [16] and significantly below (~ 300 meV) E_F for the n -type cuprates measured to date (NCCO) [17]. The flat bands would thus be expected to play a significant role in the physical properties (transport, superconductivity, etc.) of the p -type cuprates but not in the physical properties of the n types. In the rest of the paper we will make connections between the spectroscopic evidence of the flat bands and other physical properties of the cuprates, with particular attention paid to those properties which are found to be different in the n - and p -type cuprates. Although we also expect the highly nested nature of the FS of Bi 2212 to be important, the lack of a nesting feature near (π, π) in the measured FS of YBCO compels us to concentrate primarily on the flat bands. Much of this discussion assumes we can borrow the quasiparticle concept. It should be pointed out, however, that due to uncertainties regarding the photoemission line shape and background, it is still a question whether photoemission data can be interpreted using the quasiparticle concept as defined by Fermi-liquid theory.

Before exploring the possible consequences of these flat bands, we note that within the single particle approximation we can directly determine the single particle density of states $N(E_F)$ from the dispersion relationship of the quasiparticle peaks (we ignore the “background” for this discussion). The striped circles of Fig. 2(a) occupy approximately 20% of the Brillouin zone, and represent bands which lie within approximately ± 40 meV of E_F . This gives an average $N(E_F)$ for that region of $(2 \text{ states per band} \times 20\%) / (80 \text{ meV Cu site})$ or 5 states/(eV Cu site). This is much greater than the LDA results of between 1 and 2 states/(eV Cu site) [12], and is much closer to Pauli susceptibility measurements performed on very similar samples which gave an $N(E_F)$ of 7.0 states/(eV Cu site) [4] and thermodynamic measurements (specific heat discontinuity and zero temperature critical field) of YBCO₇ which gave an $N(E_F)$ of approximately 5.8 states/(eV Cu site) [18]. In contrast to this, we have low carrier concentrations inferred from the high resistivities, the Hall effect data, and chemical arguments.

Many of the discrepancies can be accounted for by the fact that the flat bands will have low electron mobilities, and so will not contribute significantly to the resistivity or Hall effect data. (Note that the two pieces of FS will also cause a cancellation of the Hall coefficient, and the temperature dependence may be related to the curvature of the FS orbits [9]).

Some examples of anomalous properties of the p -type cuprates are the T_c , which is significantly higher in the p types than in the n types, and the temperature dependence of the resistivity, which is linear over a very wide temperature range in optimally doped p types [19], but which is quadratic for NCCO [20]. The possibility that these and other anomalous properties may be related to flat bands at E_F and has been theoretically discussed in the literature, primarily within the context of a van Hove singularity in the density of states [18,21]. Finally, there is the issue of the symmetry of the superconducting order parameter. There is mounting evidence from NMR [22], ARPES [10], penetration depth [23], tunneling spectroscopy [24], infrared transmission [24], and the phase coherence of YBCO-Pb dc SQUIDS [25] that the gap in the p -type cuprates is strongly anisotropic and possibly even d wave. On the other hand, penetration depth measurements indicate an isotropic s -wave gap in the n -type superconductor NCCO [26]. It has been suggested that the n types should have a gap of similar symmetry to that found in the p types, and that the penetration depth measurements on NCCO can be understood in terms of poor sample quality [27]. The present data, in conjunction with recent experimental data on NCCO [17], clearly indicate that the electronic structure of the p - and n -type cuprates is very different. We suggest that this may be responsible for the possible differences in gap symmetry. Some theoretical work by Dickinson and Doniach supports this proposition [28]. They showed that a d -wave gap may be stabilized by a k -space anisotropy in the contribution to $N(E_F)$, with a larger gap in the region of high state density due to the energy gain from gapping many states. This is precisely what has been observed in our ARPES measurements of the SC state of Bi 2212 — $\Delta(\mathbf{k})$ is maximum near \bar{M} and minimum near the crossing along Γ - $X(Y)$ [10]. In NCCO, a strongly anisotropic or d -wave gap may not be favored since the flat bands are well below E_F .

We are grateful to critical readings by Seb Doniach and John Ruvalds. The data presented here were obtained at SSRL, which is operated by the DOE Office of Basic Energy Sciences, Division of Chemical Sciences. The office's Division of Materials Science has provided support for this research. Beam line 5 of SSRL was built with DARPA, ONR, AFOSR, AOR, DOE, and NSF support. The Stanford work was supported by NSF Grants No. DMR8913478 and No. DMR912188, and the NSF grant through the Center of Material Research.

D.S.D. acknowledges support from a DOE Distinguished Postdoctoral Research fellowship.

- [1] The superior surface quality of Bi 2212 is generally attributed to its unique crystal structure; a pair of very weakly bound BiO planes exist, between which the crystal cleaves very easily. See, for example, P. A. P. Lindberg *et al.*, Surf. Sci. Rep. **11**, No. 1-4, 1 (1990).
- [2] P. W. Anderson (to be published); Phys. Rev. Lett. **67**, 660 (1991).
- [3] J. Ruvalds *et al.* (unpublished); Phys. Rev. B **43**, 5498 (1991).
- [4] D. B. Mitzi *et al.*, Phys. Rev. B **41**, 6564 (1990); L. W. Lombardo *et al.*, J. Cryst. Growth **118**, 483 (1992).
- [5] At lower temperatures the Bi 2212 surface will collect gasses, resulting in a time-dependent superconducting gap (see Ref. [11]).
- [6] The normalization used in the presentation of all data shown in this paper is to scale all valence band spectra to have the same maximum intensity, and then apply this same scaling to the near Fermi edge spectra.
- [7] Possible origins of the background are the incoherent part of the spectrum or elastic scattering of the photoelectron.
- [8] Earlier studies in which these polarization effects were not exploited were not able to distinguish both the crossing between Γ and \bar{M} and between \bar{M} and $X(Y)$. See, for example, D. S. Dessau *et al.*, Phys. Rev. B **45**, 5095 (1992).
- [9] A. Carrington *et al.*, Phys. Rev. Lett. **69**, 2855 (1992).
- [10] Z.-X. Shen *et al.*, Phys. Rev. Lett. **70**, 1553 (1993).
- [11] D. Scalapino *et al.*, Phys. Rev. B **34**, 8190 (1986); P. Monthoux and D. Pines, Phys. Rev. Lett. **69**, 961 (1992).
- [12] S. Massida *et al.*, Physica (Amsterdam) **152C**, 251 (1988).
- [13] M. Tanaka *et al.*, Nature (London) **339**, 691 (1989); T. Hasegawa *et al.*, Jpn. J. Appl. Phys. **29**, L434 (1990).
- [14] B. O. Wells *et al.*, Phys. Rev. Lett. **65**, 3056 (1990).
- [15] See Fig. 1(a) and C. G. Olsen *et al.*, Phys. Rev. B **42**, 381 (1990).
- [16] R. Liu *et al.*, Phys. Rev. B **45**, 5614 (1992); J. Tobin *et al.*, Phys. Rev. B **45**, 5563 (1992); D. M. King *et al.* (unpublished); K. Gofron *et al.* (unpublished).
- [17] D. M. King *et al.*, Phys. Rev. Lett. **70**, 3159 (1993).
- [18] C. C. Tsuei *et al.*, Phys. Rev. Lett. **69**, 2134 (1992).
- [19] M. Gurvitch *et al.*, Phys. Rev. Lett. **59**, 1337 (1987).
- [20] S. J. Hagen *et al.*, Phys. Rev. B **43**, 13606 (1991).
- [21] J. Labbe and J. Bok, Europhys. Lett. **3**, 1225 (1987); R. S. Markiewicz, Physica (Amsterdam) **153-155C**, 1181 (1988).
- [22] P. C. Hammel *et al.*, Phys. Rev. Lett. **63**, 1992 (1989).
- [23] W. Hardy *et al.* (unpublished).
- [24] D. Mandrus *et al.*, Phys. Rev. Lett. **70**, 2629 (1993).
- [25] D. A. Wollman *et al.* (unpublished).
- [26] D. H. Wu *et al.*, Phys. Rev. Lett. **70**, 85 (1993).
- [27] P. A. Lee (unpublished).
- [28] P. H. Dickinson and S. Doniach, Phys. Rev. B **47**, 11447 (1993).